2

Conf-910414--14

UCRL-JC--104789

DE91 007598

ANALYSIS OF SPHERICAL GEOMETRY FINITE ELEMENT TRANSPORT SOLUTIONS IN THE THICK DIFFUSION LIMIT

Todd S. Palmer
Dept of Nuclear Engineering
Cooley Bldg.. North Campus
University of Michigan
Ann Arbor, MI 48103

Marvin L. Adams
Lawrence Livermore National Laboratory
P.O. Box 808, L-18
Livermore, CA 94550

This paper was prepared for submittal to
THE AMERICAN NUCLEAR SOCIETY INTERNATIONAL TOPICAL MEETING
Pittsburgh, PA
April 28 - May 1, 1991

January 15, 1991

Analysis of Spherical Geometry Finite Element Transport Solutions in the Thick Diffusion Limit

Todd S. Palmer
Dept. of Nuclear Engineering
Cooley Bldg., North Campus
University of Michigan
Ann Arbor, MI 48103

Marvin L. Adams
Lawrence Livermore National Laboratory
P.O. Box 808, L-18
Livermore, CA 94550

Abstract

An asymptotic analysis is performed on a *family* of discontinuous finite element methods (DFEMs) for spherical geometry transport. It is found that transport methods of this type transition into discrete versions of the spherical geometry diffusion equation in the thick diffusion limit with boundary conditions that may, in general, be inaccurate. A linear DFEM method has been designed such that its asymptotic diffusion boundary conditions are accurate. In a related development, the asymptotic diffusion equation is used to accelerate the transport calculation and the iterative scheme is fully described. The results of the analysis are confirmed by numerical testing of the specific case of linear elements.

I. Introduction

Recently, much work has been done in developing transport methods that are accurate in optically thick, diffusive regions[1-3]. Realistic problems in thermal radiation transport often contain regions of this type. The main emphasis is the design of schemes that allow the use of spatial grids whose cells are thick compared ~ a mean-free path in these regions. Our interest is in constructing discontinuous finite element methods (DFEMs) for spherical geometry transport (1-D) that are accurate for diffusive problems.

The first component of our design is an asymptotic analysis of the transport equation, which previously has been performed only in rectilinear geometries. We perform this analysis on an entire family of DFEMs in spherical geometry. Numerical testing follows, in which we consider the special instance of linear elements. We discover that in thick, diffusive regions, every spherical geometry DFEM produces a solution that (to leading order) satisfies a discrete diffusion equation. This is a highly desirable result, for we know that in the interior of such regions the exact transport solution (to leading order) satisfies a diffusion equation. Despite this, we find that in general the spherical geometry DFEM solution can be inaccurate in diffusive regions, because it satisfies boundary conditions that in general can be inaccurate. We find that, for the the case of linear elements, the boundary conditions are inaccurate when using coarse spatial grids on small spheres.

We are also interested in utilizing the diffusion equation resulting from this analysis in a

synthetic acceleration scheme for iteratively solving the spherical geometry DFEM equations. Currently, we are using a combined Asymptotic - P_1 acceleration technique which we fully describe. This technique is essentially the same as that presented by Wareing and Larsen[4].

II. Asymptotic Analysis

First, we will look at the behavior of the exact spherical geometry transport solution in a diffusive region. We write the conservative form of the monoenergetic spherical geomety transport equation, assuming isotropic sources and scattering, as:

$$\mu \frac{\partial}{\partial r} r^2 \Psi(r,\mu) + r \frac{\partial}{\partial \mu} (1-\mu^2) \Psi(r,\mu) + r^2 \sigma_t \Psi(r,\mu) = \frac{r^2}{2}(\sigma_t - \sigma_a)\Phi(r) + \frac{r^2}{2} Q(r), \qquad r_{in} < r < r_{out}, \tag{1a}$$

$$\Psi(r,\mu) = \begin{cases} F(\mu), & r = r_{in}, \ \mu > 0 \\ G(\mu), & r = r_{out}, \ \mu < 0 \end{cases}, \tag{1b}$$

where

$\Psi(r,\mu)$ = angular flux at radius r, direction μ,
$\Phi(r)$ = scalar flux at radius r

$$= \int_{-1}^{1} d\mu \, \Psi(r,\mu)$$

$F(\mu)$ = angular flux incident on inner boundary,
$G(\mu)$ = angular flux incident on outer boundary,
$\sigma_t(r)$ = total cross section at radius r,
$\sigma_a(r)$ = absorption cross section at radius r,
$Q(r)$ = inhomogeneous source.

In order to analyze the behavior of this equation in thick diffusive regions, we write the problem in dimensionless form and introduce a scaling parameter ε that measures the degree to which the problem is diffusive. Our *scaled* transport equation has the form,

$$\mu \frac{\partial}{\partial r} r^2 \Psi(r,\mu) + r \frac{\partial}{\partial \mu} (1-\mu^2) \Psi(r,\mu) + r^2 \frac{\sigma_t}{\varepsilon} \Psi(r,\mu) = \frac{r^2}{2}\left(\frac{\sigma_t}{\varepsilon} - \varepsilon\sigma_a\right)\Phi(r) + \frac{r^2}{2}\varepsilon Q(r), \qquad r_{in} < r < r_{out}, \tag{2}$$

and we observe the character of the solution as ε tends towards zero. We find that in the interior of the diffusive region the solution satisfies the following conditions:

$$\Psi(r,\mu) = \frac{1}{2}\Phi(r) + O(\varepsilon), \quad r \text{ away from the boundaries}, \tag{3a}$$

$$-\frac{1}{r^2}\frac{\partial}{\partial r}\frac{1}{3\sigma_t} r^2 \frac{\partial}{\partial r}\Phi(r) + \sigma_a \Phi(r) = Q(r), \tag{3b}$$

$$\Phi(r_{in}) = \int_0^1 d\mu \, W(\mu) \, F(\mu), \tag{3c}$$

$$\Phi(r_{out}) = \int_{-1}^{0} d\mu\, W(-\mu)\, G(\mu) \quad . \tag{3d}$$

Note that both boundary conditions are Dirichlet conditions equal to weighted integrals of the incoming intensity. The weight function W is defined in terms of Chandrasekhar's H function for a purely scattering medium[5]:

$$W(\mu)=\frac{\sqrt{3}}{2}\mu H(\mu) \quad . \tag{4}$$

W can be approximated by a simple polynomial:

$$\begin{aligned} W(\mu) &= 0.956\mu + 1.565\mu^2 \pm 0.0035 \\ &\approx \mu + 1.5\mu^2 \quad . \end{aligned} \tag{5}$$

We now look at the DFEM discretized spherical geometry transport equations. We start with the S_N analog of equation (1a):

$$\begin{aligned} \mu_m \frac{\partial}{\partial r} r^2 \Psi_m(r) + r\left[\frac{\alpha_{m+1/2}\Psi_{m+1/2}(r) - \alpha_{m-1/2}\Psi_{m-1/2}(r)}{w_m}\right] + \sigma_t r^2 \Psi_m(r) \\ = \frac{r^2}{2}(\sigma_t - \sigma_a)\Phi(r) + \frac{r^2}{2} Q(r) \quad , \; m=1,\cdots,N \end{aligned} \tag{6a}$$

$$\begin{aligned} \Psi_m(r_{in}) &= F(\mu_m)=F_m \quad , \; for \;\; \mu_m > 0 \\ \Psi_m(r_{out}) &= G(\mu_m)=G_m \quad , \; for \;\; \mu_m < 0 \end{aligned} \tag{6b}$$

where

μ_m , w_m = angles and weights of the quadrature set , $m=1,\cdots,N$,

$\alpha_{m-1/2}$, $\alpha_{m+1/2}$ = angular derivative differencing coefficients ,

$\Psi_m(r)$ = angular flux at radius r, direction μ_m,

$\Phi(r)$ = scalar flux at radius r $= \sum_{m=1}^{N} w_m \Psi_m(r)$.

At this point, we specify a spatial grid that breaks the problem into K regions,

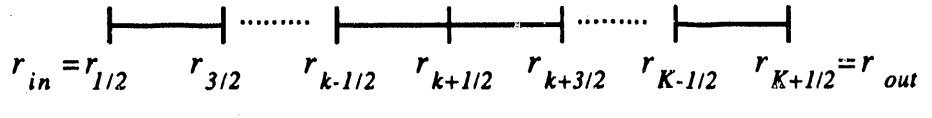

and in each k^{th} region choose a set of weight functions $\{v_{ki}(r),\ 1\le i\le J_k\}$ and basis functions $\{b_{kj}(r),\ 1\le j\le J_k\}$. The weight and basis functions are assumed to be continuous within each region, but may be discontinuous at region edges. The weight and basis functions associated with a given region are assumed to vanish outside that region. We can now derive the DFEM form of the equations in four steps:

1) Multiply the transport equation (6) by a weight function, $v_{ki}(r)$ and integrate

over the k^{th} region volume. Convert the integral of the leakage term into a surface integral using Green's theorem. The resulting equation is:

$$\begin{aligned}
&\mu_m\left[\nu_{ki}(r_{k+1/2})r_{k+1/2}^2\psi_m(r_{k+1/2})-\nu_{ki}(r_{k-1/2})r_{k-1/2}^2\psi_m(r_{k-1/2})\right] \\
&\quad + \int_{r_{k-1/2}}^{r_{k+1/2}} dr\ r\ \nu_{ki}\left[\frac{\alpha_{m+1/2}\Psi_{m+1/2}-\alpha_{m-1/2}\Psi_{m-1/2}}{w_m}\right] \\
&\quad - \mu_m\int_{r_{k-1/2}}^{r_{k+1/2}} dr\, r^2\ \psi_m\frac{d}{dr}\nu_{ki} \ + \int_{r_{k-1/2}}^{r_{k+1/2}} dr\, r^2\ \sigma_t\psi_m\ \nu_{ki} \\
&\quad = \int_{r_{k-1/2}}^{r_{k+1/2}} dr\, r^2\ \nu_{ki}\left[(\sigma_t-\sigma_a)\frac{\phi}{2}+\frac{q}{2}\right] \quad .
\end{aligned} \tag{7}$$

2) Replace quantities on region edges (where they can be discontinuous) by their *upstream* values:

$$\psi_m(r_{k+1/2}) = \begin{cases} \psi_m(r_{k+1/2}^+) \text{ , for } \mu_m < 0 \\ \psi_m(r_{k+1/2}^-) \text{ , for } \mu_m > 0 \end{cases} \tag{8}$$

where

$r_{k+1/2}^+$ is located just to the right of $r_{k+1/2}$ (just *outside* the kth region)
$r_{k+1/2}^-$ is located just to the left of $r_{k+1/2}$ (just *inside* the kth region).

3) Approximate the unknowns and sources as expansions in basis functions:

$$\begin{aligned}
\Psi_m(r) \approx \psi_m(r) &\equiv \sum_{k=1}^{K}\sum_{j=1}^{J_k}\psi_{mkj}b_{kj}(r) \quad , \\
\Phi(r) \approx \phi(r) &\equiv \sum_{k=1}^{K}\sum_{j=1}^{J_k}\phi_{kj}b_{kj}(r) \quad , \\
Q(r) \approx q(r) &\equiv \sum_{k=1}^{K}\sum_{j=1}^{J_k}q_{kj}b_{kj}(r) \quad .
\end{aligned} \tag{9}$$

4) Define the following matrices and vectors:

$$\begin{aligned}
(\mathbf{L}_k)_{i,j} &\equiv -\int_{r_{k-1/2}}^{r_{k+1/2}} dr\, r^2\,\frac{d}{dr}\nu_{ki}(r)\ b_{kj}(r) \\
(\mathbf{R}_k)_{i,j} &\equiv \int_{r_{k-1/2}}^{r_{k+1/2}} dr\ r\ \nu_{ki}(r)\ b_{kj}(r)
\end{aligned}$$

$$(\mathbf{T}_k)_{i,j} \equiv \int_{r_{k-1/2}}^{r_{k+1/2}} dr\ r^2\, \nu_{ki}(r)\, b_{kj}(r)$$

$$\underline{\psi}_{mk} \equiv [\psi_{mk1}, \cdots, \psi_{mkJ_k}]^t$$
$$\underline{\phi}_k \equiv [\phi_{k1}, \cdots, \phi_{kJ_k}]^t$$
$$\underline{q}_k \equiv [q_{k1}, \cdots, q_{kJ_k}]^t$$

This gives us the spherical geometry discrete-ordinates general DFEM transport equation:

$$\mu_m\left[\underline{\nu}_k(r_{k+1/2})r_{k+1/2}^2\psi_m(r_{k+1/2}^-)-\underline{\nu}_k(r_{k-1/2})r_{k-1/2}^2\psi_m(r_{k-1/2}^+)\right]$$
$$+\ \mu_m\mathbf{L}_k\underline{\psi}_{mk}+\mathbf{R}_k\left[\frac{\alpha_{m+1/2}\underline{\psi}_{m+1/2k}-\alpha_{m-1/2}\underline{\psi}_{m-1/2k}}{w_m}\right]+\sigma_{tk}\mathbf{T}_k\underline{\psi}_{mk} \qquad (10)$$
$$=(\sigma_{tk}-\sigma_{ak})\frac{\mathbf{T}_k}{2}\underline{\phi}_k+\frac{\mathbf{T}_k}{2}\underline{q}_k \quad , \ m=1,\cdots,N \quad , \ \mu_m \gtrless 0 \quad , \ k=1,\cdots,K \ .$$

To begin the asymptotic analysis of the discretized problem, we must scale the DFEM equation in a way consistent with the scaling of the analytic transport equation (2). We fix the spatial grid as we let ε go to zero, so that we are investigating what is known as the "thick" diffusion limit, or the limit as each spatial region becomes thick compared to a mean free path. Now we assume our solution to be an asymptotic expansion in powers of ε, and observe the behavior of the leading-order terms as ε shrinks to zero. The result is that the leading-order scalar flux is continuous in the problem interior and satisfies the following diffusion equation:

$$\left[-\mathbf{D}_k\mathbf{L}_k\mathbf{T}_k^{-1}(\mathbf{L}_k-2\mathbf{R}_k+\mathbf{V}_k)\underline{\phi}_k^{(0)}+\sigma_{ak}\mathbf{T}_k\underline{\phi}_k^{(0)}\right]_{J_k}$$
$$+\left[-\mathbf{D}_{k+1}\mathbf{L}_{k+1}\mathbf{T}_{k+1}^{-1}(\mathbf{L}_{k+1}-2\mathbf{R}_{k+1}+\mathbf{V}_{k+1})\underline{\phi}_{k+1}^{(0)}+\sigma_{ak+1}\mathbf{T}_{k+1}\underline{\phi}_{k+1}^{(0)}\right]_1 \qquad (11a)$$
$$=\left[\mathbf{T}_k\underline{q}_k\right]_{J_k}+\left[\mathbf{T}_{k+1}\underline{q}_{k+1}\right]_1 \quad , \ 1\le k\le K-1 \quad ,$$

and

$$\left[-\mathbf{D}_k\mathbf{L}_k\mathbf{T}_k^{-1}(\mathbf{L}_k-2\mathbf{R}_k+\mathbf{V}_k)\underline{\phi}_k^{(0)}+\sigma_{ak}\mathbf{T}_k\underline{\phi}_k^{(0)}\right]_j=\left[\mathbf{T}_k\underline{q}_k\right]_j \ , \qquad (11b)$$
$$1\le k\le K \quad , \quad 1<j<J_k \ .$$

where

$$\mathbf{D}_k = \text{diffusion coefficient} \equiv \frac{1}{3\sigma_{tk}} \ ,$$

$$(\mathbf{V}_k)_{i,j}=\begin{cases} -r_{k-1/2}^2 \ , \ i=1, j=1 \\ r_{k+1/2}^2 \ , \ i=J_k, j=J_k \qquad 1\le i,j\le J_k \\ 0 \ , \ \text{otherwise} \end{cases}$$

Note that Eq. (11a) includes information from two adjoining regions, whereas Eq. (11b) is local to

the k^{th} region; for linear elements, $J_k = 2$ and Eq. (11a) is our only diffusion equation. With this equation we obtain our first major result: the general DFEM discrete-ordinates spherical geometry transport equation goes over to a diffusion equation which is a discretized version of Eq. (3b) in the limit as the spatial regions become optically thick. The boundary conditions associated with this diffusion equation are found to be:

$$\psi_m^{(0)}(r_{in}) = \frac{1}{2}\phi^{(0)}(r_{in}) = \sum_{\mu_m > 0} w_m \, W_{D,\,in}(\mu_m) F_m$$
$$\psi_m^{(0)}(r_{out}) = \frac{1}{2}\phi^{(0)}(r_{out}) = \sum_{\mu_m < 0} w_m \, W_{D,\,out}(|\mu_m|) G_m \, . \tag{12}$$

These are discrete-ordinates representations of Dirichlet conditions, where the weight functions are defined by

$$W_{D,\,in}(\mu_m) = (1-\alpha)\left[\frac{2}{\rho}\mu_m\right] + \alpha\left[\frac{1}{\rho}\mu_m + \frac{3}{2}\mu_m^2\right]$$
$$W_{D,\,out}(\mu_m) = (1-\beta)\left[\frac{2}{\rho}\mu_m\right] + \beta\left[\frac{1}{\rho}\mu_m + \frac{3}{2}\mu_m^2\right] \tag{13a}$$

$$\rho = \sum_{\mu_m > 0 \text{ or } \mu_m < 0} 2|\mu_m| w_m \approx 1 \, . \tag{13b}$$

α and β are determined by the particular DFEM in use, and depend on the width of the region adjoining the boundary and the spatial position of the boundary. Notice that the most accurate approximation of the analytic boundary conditions occurs when α and β are near 1. If α and β are near zero, the discrete boundary conditions will be poor approximations to the analytic boundary conditions. Also, if the incident angular flux at the boundary is isotropic, both boundary conditions go over to the analytic result, independent of α and β. We have our second main result: the boundary conditions associated with the asymptotic diffusion equation can be inaccurate in some cases.

We will now turn our attention to some representative DFEM schemes, namely the linear DFEM (derived using linear basis and weight functions) and the lumped mass-matrix linear DFEM. It can be shown that α and β satisfy the following equations for the lumped mass-matrix linear DFEM:

$$\alpha = \frac{3\eta^2}{1+\eta+\eta^2} \tag{14a}$$

$$\beta = \frac{3}{1+\eta+\eta^2} \tag{14b}$$

where η is given by

$$\eta = \frac{\text{region inner radius}}{\text{region outer radius}} \, . \tag{14c}$$

Notice that as η approaches 1 (the slab geometry limit) both α and β go to 1 and the boundary conditions are accurate. However, when η is small, the boundary conditions will be inaccurate.

This corresponds to the situations where we are solving problems on geometrically small spheres with coarse spatial regions. Without mass-matrix lumping, the equations for α and β are more complicated and the corresponding boundary conditions are considerably less accurate[3].

We would like a DFEM transport method that limits to a reasonable diffusion equation with boundary conditions that are always accurate. By perturbing the linear DFEM system of equations we have designed a method for which α and β are equal to 1 in all cases. This new method has the same $\mathbf{T}_k$ and $\mathbf{V}_k$ matrices as in the lumped mass-matrix linear DFEM, but the $\mathbf{L}_k$ and $\mathbf{R}_k$ matrices are defined in this way:

$$\mathbf{L}_k = \frac{r_{k+1/2}^2}{12}\begin{bmatrix} 1+2\eta_k+3\eta_k^2 & \eta_k^2(3+2\eta_k+\eta_k^2) \\ -(1+2\eta_k+3\eta_k^2) & -\eta_k^2(3+2\eta_k+\eta_k^2) \end{bmatrix} \tag{15a}$$

$$\mathbf{R}_k = \frac{r_{k+1/2}^2(1-\eta_k)}{24(1+\eta_k)}\begin{bmatrix} 1+4\eta_k+5\eta_k^2 & -\eta_k^2(5+4\eta_k+\eta_k^2) \\ 3+8\eta_k+3\eta_k^2 & (8+12\eta_k+9\eta_k^2+4\eta_k^3+\eta_k^4) \end{bmatrix} \tag{15b}$$

with

$$\eta_k = \frac{r_{k-1/2}}{r_{k+1/2}}.$$

We obtain this result by requiring that our method have three properties: 1) the method should satisfy particle balance, 2) the infinite medium transport solution should be preserved, and 3) the resulting asymptotic diffusion boundary conditions should have the accurate weight function.

III. Asymptotic-P_1 Diffusion Synthetic Acceleration

In this section we describe the iterative technique used to solve the optically thick, diffusive problems we are interested in. We will concentrate on the case of linear DFEMs only. The acceleration scheme has three steps (l is the iteration index):

1) Transport sweep: with a previous estimate for the scalar flux, perform one full transport source iteration,

$$\begin{aligned} &\mu_m\left[\underline{\nu}_k(r_{k+1/2})r_{k+1/2}^2\psi_m^{(l+1/2)}(r_{k+1/2}^-)-\underline{\nu}_k(r_{k-1/2})r_{k-1/2}^2\psi_m^{(l+1/2)}(r_{k-1/2}^+)\right] \\ &+\mu_m\mathbf{L}_k\underline{\psi}_{mk}^{(l+1/2)}+\mathbf{R}_k\left[\frac{\alpha_{m+1/2}\underline{\psi}_{m+1/2k}^{(l+1/2)}-\alpha_{m-1/2}\underline{\psi}_{m-1/2k}^{(l+1/2)}}{w_m}\right]+\sigma_{tk}\mathbf{T}_k\underline{\psi}_{mk}^{(l+1/2)} \\ &=(\sigma_{tk}-\sigma_{ak})\frac{\mathbf{T}_k}{2}\underline{\phi}_k^{(l)}+\frac{\mathbf{T}_k}{2}\underline{q}_k \quad , m=1,\cdots,N \quad , \mu_m \gtrless 0 \quad , k=1,\cdots,K \end{aligned} \tag{16a}$$

$$\underline{\phi}_k^{(l+1/2)} = \sum_{m=1}^{N} w_m\underline{\psi}_{mk}^{(l+1/2)} \tag{16b}$$

2) Asymptotic diffusion acceleration: we solve the asymptotic diffusion equation for *continuous* updates to the scalar flux,

$$\left[-D_k L_k T_k^{-1}(L_k - 2R_k + V_k) f_k^{(l+1/2)} + \sigma_{ak} T_k f_k^{(l+1/2)}\right]_{J_k}$$

$$+\left[-D_{k+1} L_{k+1} T_{k+1}^{-1}(L_{k+1} - 2R_{k+1} + V_{k+1}) f_{k+1}^{(l+1/2)} + \sigma_{ak+1} T_{k+1} f_{k+1}^{(l+1/2)}\right]_1$$

$$= \left[(\sigma_{tk} - \sigma_{ak})\, T_k\left(\underline{\phi}_k^{(l+1/2)} - \underline{\phi}_k^{(l)}\right)\right]_{J_k} + \left[(\sigma_{tk+1} - \sigma_{ak+1})\, T_{k+1}\left(\underline{\phi}_{k+1}^{(l+1/2)} - \underline{\phi}_{k+1}^{(l)}\right)\right]_1 , \qquad (16c)$$

$$1 \le k \le K-1$$

3) P1 mapping of updates: we apply the P_1 approximation to our transport equation and obtain a way of mapping the asymptotic diffusion updates back into a *discontinous* representation,

$$f_k^{(l+1)} = Y_k^{-1}\left[Z_k f_k^{(l+1/2)} + (\sigma_{tk} - \sigma_{ak})\, T_k\left(\underline{\phi}_k^{(l+1/2)} - \underline{\phi}_k^{(l)}\right)\right] ,$$

$$Y_k = -D_k(L_k + V_k)T_k^{-1}(L_k - 2R_k) + V_k \begin{bmatrix} -\bar{\mu} & 0 \\ 0 & \bar{\mu} \end{bmatrix} + \sigma_{ak} T_k , \qquad (16d)$$

$$Z_k = D_k(L_k + V_k)T_k^{-1} V_k + V_k \begin{bmatrix} -\bar{\mu} & 0 \\ 0 & \bar{\mu} \end{bmatrix} ,$$

where

$$\bar{\mu} = \sum_{\mu_m > 0 \text{ or } \mu_m < 0} |\mu_m| w_m$$

$$\underline{\phi}_k^{(l+1)} = \underline{\phi}_k^{(l+1/2)} + f_k^{(l+1)} \qquad (16e)$$

The direct coupling of the angular and spatial variables in spherical geometry prohibits us from performing a Fourier analysis of this acceleration scheme. We have, however, numerically studied the convergence performance of the linear DFEM, lumped mass-matrix DFEM, and our new method. We will present these results in the next section.

IV. Numerical Results

In this section we present the results of numerical tests designed to 1) substantiate the claims of our asymptotic analysis and 2) illustrate the convergence behavior of the acceleration schemes. To confirm the asymptotic analysis results, we consider two spherical geometry test problems, both of which contain thick diffusive regions. Each problem is solved with the linear DFEM, lumped-mass-matrix linear DFEM, and the new method, and we use the S_{16} Gauss-Legendre quadrature set. Both problems are solved using a diffusion synthetic acceleration (DSA) technique described in the previous section.

In our first test problem we simulate a purely-scattering shell 1000 mean-free paths thick surrounding a small purely-absorbing sphere. Our system is void of sources and there is an isotropically incident flux on the outside surface. We generate a reference solution using the linear DFEM with a very fine spatial mesh, and coarse-mesh (10 region) solutions with linear DFEM, lumped linear DFEM, and the new method. In purely-scattering cases, we expect the lumped and unlumped linear DFEM solutions to be the same to leading order. Our results are shown in Figure 1. We see that all methods perform very well, as our analysis predicts, because their boundary

conditions are correct for isotropically incident fluxes.

Our second test problem is a purely-scattering, source-free, 1000 mean-free-path thick sphere with an incoming flux on the outside surface that is a delta-function in angle at m ª 0.1. Results are given in Figure 2. We obtain our reference solution as before, and generate solutions for 2 regions and 10 regions with both the linear DFEM and the new method. The new method obtains the same interior solution regardless of the number of regions, as the analysis suggests; this interior solution is accurate compared to the reference solution. The solution in the outermost region is incorrect; this, too, is precisely predicted by our analysis. (In fact, our analysis predicts that *all* DFEMs will produce the same solution at the problem boundary.) With 2 regions the linear DFEM solution is low in the interior by a factor of 2. For this mesh, b ª 1.7, and W_{LD} $/W_{analytic}$ ª 0.5, explaining why the interior solution is low. The 10 region solution compares well with the reference, as b ª 1.1, and W_{LD} $/W_{analytic}$ ª 0.9. In short, our numerical tests are in precise agreement with our asymptotic analysis.

Turning now to the convergence behavior of the acceleration algorithm, we focus on homogeneous, purely-scattering (c =1) spheres at least 50 mean-free-paths (*mfp*) thick, solved using various spatial grids. The results are presented in Table 1.

Table 1. Estimated Spectral Radius for Spherical Geometry DFEM schemes, c=1, Isotropic Scattering

Δr (*mfp*)	Linear DFEM (LDFEM)	Lumped mass-matrix LDFEM	New LDFEM
0.01	0.224	0.223	0.965
0.03	0.224	0.225	0.889
0.1	0.225	0.226	0.645
0.3	0.225	0.290	0.204
1.0	0.223	0.346	0.511
3.0	0.186	0.204	0.808
10.0	0.089	0.084	0.958
30.0	0.034	0.031	0.979
100.0	0.011	0.010	0.991

We find excellent performance for both the linear and lumped mass-matrix linear DFEMs, but unacceptably poor behavior for the new scheme. Because of the new method's convergence properties, we are forced to discard it as a viable way of solving practical transport problems, at least until we are able to formulate a better iterative scheme.

IV. Conclusions

We have performed an asymptotic analysis on a *family* of discontinuous finite element methods for the spherical geometry transport equation, in an effort to understand their behavior in thick diffusive regions. We have found that in these regions, the numerical solution satisfies a discretization of the proper diffusion equation. For the case of conventional linear elements, we see that the diffusion boundary conditions imposed on the numerical solution are accurate for the most part, but can be inaccurate when the spatial cells are large and the system under consideration is small. By perturbing the linear DFEM equations, we have designed a method that limits to a reasonable diffusion equation with correct boundary behavior, regardless of the problem. However, we do not expect this new method to be useful for practical problems until an acceleration scheme with more desirable convergence properties is implemented. We have tested the methods numerically, and our results corroborate the findings of our asymptotic analysis.

Acknowledgement

Part of this work was performed under the auspices of the U.S. Department of Energy by Lawrence Livermore National Laboratory under Contract #W-7405-Eng-48.

References

1. M.L. Adams, "Discontinuous Finite-Element Transport Solutions in the Diffusion Limit in Cartesian Geometry," submitted to this conference.

2. E.W. Larsen, J.E. Morel, and W.F. Miller, Jr., *J. Comput. Physics*, **69**, p. 283 (1987).

3. E.W. Larsen and J.E. Morel, *J. Comput. Physics*, **83**, p. 212 (1989). [See also the corrigendum to appear in *J. Comput. Physics*.]

4. T.A. Wareing, E.W. Larsen, and M.L. Adams, "Diffusion Accelerated Discontinuous Finite Element Schemes for the S_N Equations in Slab and X,Y Geometries" submitted to this conference.

5. S. Chandrasekhar, *Radiative Transfer*, Dover, New York (1960).

Figure 1. Results from Test Problem 1.

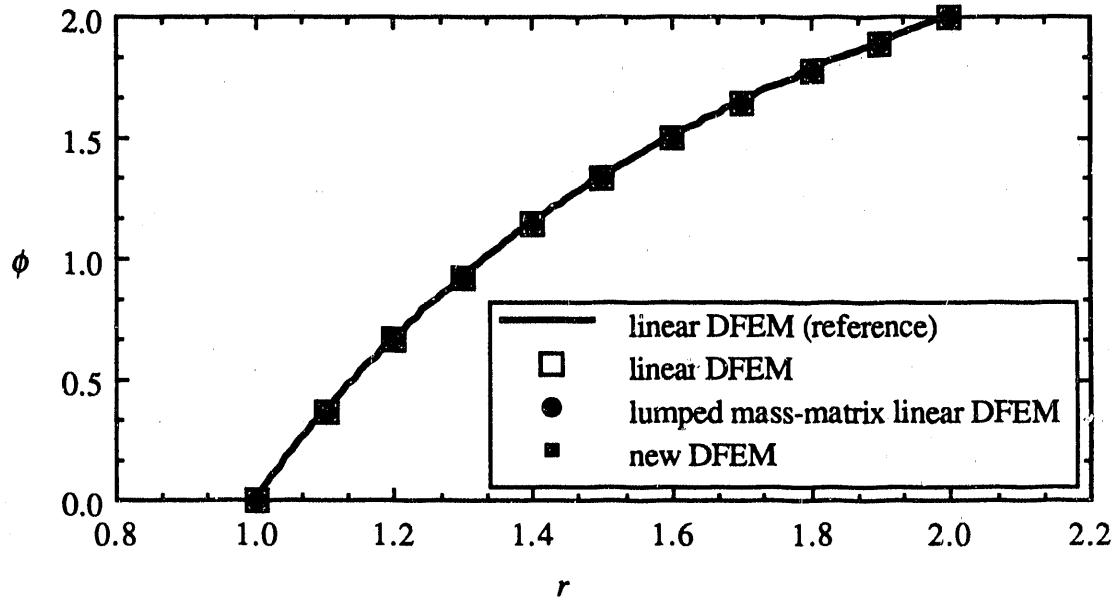

Figure 2. Results from Test Problem 2.

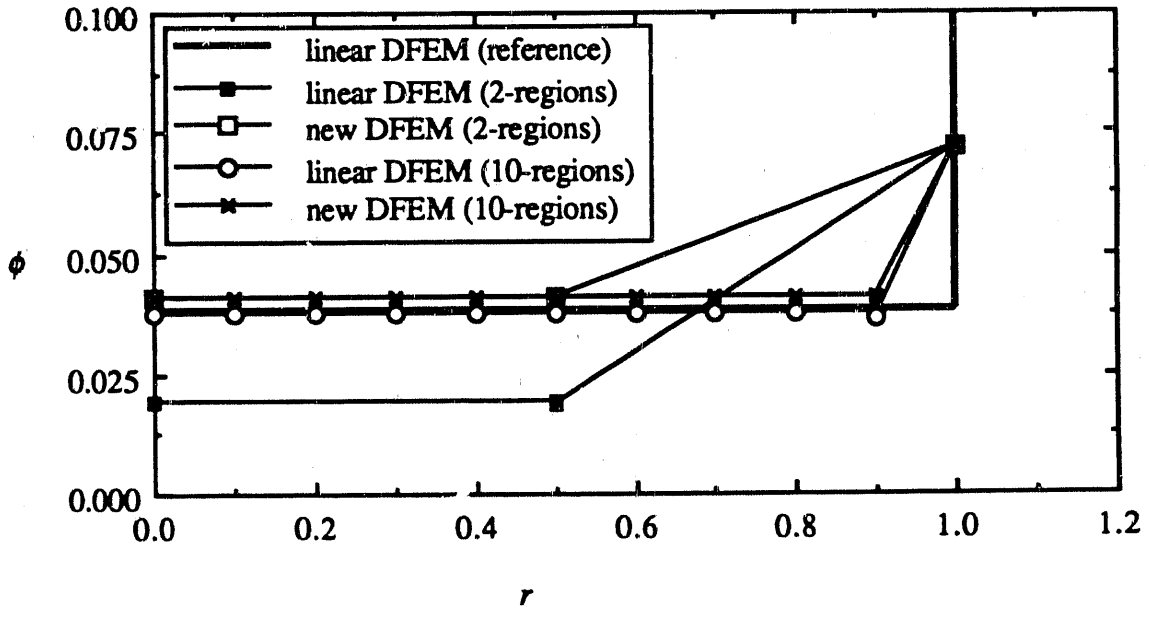

END

DATE FILMED

03 / 06 / 91